Cesium encapsulation in single-walled carbon nanotubes via plasma ion irradiation: Application to junction formation and *ab initio* investigation

G. -H. Jeong,[1,*] A. A. Farajian,[2] R. Hatakeyama,[1] T. Hirata,[1] T. Yaguchi,[3] K. Tohji,[4] H. Mizuseki,[2] and Y. Kawazoe[2]
[1] *Department of Electronic Engineering, Tohoku University, Sendai 980-8579, Japan*
[2] *Institute for Materials Research, Tohoku University, Sendai 980-8577, Japan*
[3] *Application Technology Dept., Hitachi Science System, Hitachinaka-shi 312-8504, Japan*
[4] *Department of Geoscience and Technology, Tohoku University, Sendai 980-8579, Japan*
(Received 19 May 2003; published 21 August 2003)

Using an approach different from the conventional vapor doping methods, Cs positive ions in a magnetized-plasma column are irradiated upon a negatively biased substrate which is covered with dispersed single-walled carbon nanotubes (SWNTs). The Cs ions are evidently observed inside SWNTs by the *Z*-contrast method in scanning transmission electron microscopy, demonstrating the formation of alkali-metal encapsulating SWNTs. *Ab initio* band structures and density of states for the light and heavy doping regimes indicate the possibility of using Cs-doped SWNTs as doped junctions, with potential application in nanoelectronics. This is supported by the direct experimental observation of an actual junction.

DOI: 10.1103/PhysRevB.68.075410 PACS number(s): 61.80.Lj, 81.07.De, 68.37.Lp, 71.15.Mb

I. INTRODUCTION

Accommodation of various dopant atoms, molecules, and compounds can be used to modify the intrinsic electronic and mechanical properties of carbon nanotubes.[1–3] Among these, in particular, alkali metal intercalation (Li, K, Rb, and Cs) has been very actively investigated and rapidly progressed.[4–6] Suzuki *et al.*[7,8] were the first to report the intercalation-induced structural disorder. They also observed a drastic decrease of the work function in the Cs-intercalated single-walled carbon nanotubes (SWNTs). The major methods of intercalation that have been used up to now consist of vapor deposition by thermally diffused gas, capillary wetting of liquid phase, or direct soaking in the solution. These methods inevitably give rise to structural disorder, namely, structural instability at ambient surroundings due to their inherent air-sensitive property. Therefore, in order to realize the insertion of alkali metals inside the nanotubes, in contrast to the interstitial doping, these methods need substantial improvement through, e.g., intercalant-flux or dopant-drift energy control. Furthermore, the fact that only one species can be intercalated at one process is a critical barrier to more intricate applications, such as P-N nanoscale device as predicted by the theoretical calculations.[9,10]

In this paper, we mainly focus on the elucidation of Cs-encapsulating SWNTs. The experimental observations are accompanied by *ab initio* calculations in order to obtain a more accurate/quantitative understanding of the experimental results. As a new experimental approach, we make use of the plasma ion irradiation method, where differently charged ions could be *selectively* encapsulated inside the same sample, just by changing the polarity of applied bias. Although some works have reported encapsulation of alkali metals in fullerene cages via ion-beam method,[11,12] and high-energy ion-beam injection of He into charged fullerenes,[13–15] the present work reports on encapsulation of an alkali metals, i.e, Cs, in single-walled carbon nanotubes.

II. EXPERIMENTAL AND THEORETICAL APPROACHES

A. Experimental

SWNTs were prepared by electric-arc discharge method. Typical bundle-type and sea-urchin type nanotubes are produced using Fe-Ni and Se catalysts, mixed in an anode graphite rod, respectively. A SWNT paper purified by the HIDE method[16] was dispersed by brief sonication in ethanol and then droplets of this suspension were doped and dried on stainless steel substrate. The details of the Cs plasma production are similar to that of other alkali plasmas,[17] which takes place by surface contact ionization. Subsequent plasma ion irradiation is carried out for 1 h in a vacuum chamber schematically shown in Fig. 1(a), where the plasma is radially confined by a magnetic field ($\mathbf{B}=2$ kG) between a plasma-source electrode (hot plate) and an axially terminating end-plate, and its parameters are measured by a Langmuir probe. When negative dc bias voltages ($\phi_{ap}<0$) are applied to the substrate in the plasma with respect to the grounded plasma-source electrode (hot plate), positive Cs ions ($n_i \geqslant 1 \times 10^{-10}$ cm^{-3}; n_i: ion density) are substantially accelerated by plasma sheaths in front of the substrate and finally bombard the SWNTs.

B. Theoretical

We perform *ab initio* calculations in order to obtain a more clear insight about the physics of the experimental results. The *ab initio* approach employed here is based on the generalized gradient approximation (GGA) to density functional theory. Norm-conserving pseudopotentials[18] are used to present core electrons, while valence electrons are described using numerical atomic orbitals as basis sets. Here we use split-valence double-ζ basis sets, plus polarization orbitals. As for the GGA exchange-correlation functional, the Perdew-Burke-Ernzerhof (PBE) parametrization,[19] is used. Direct diagonalization is employed to solve for the electronic structure. The same general *ab initio* scheme, implemented

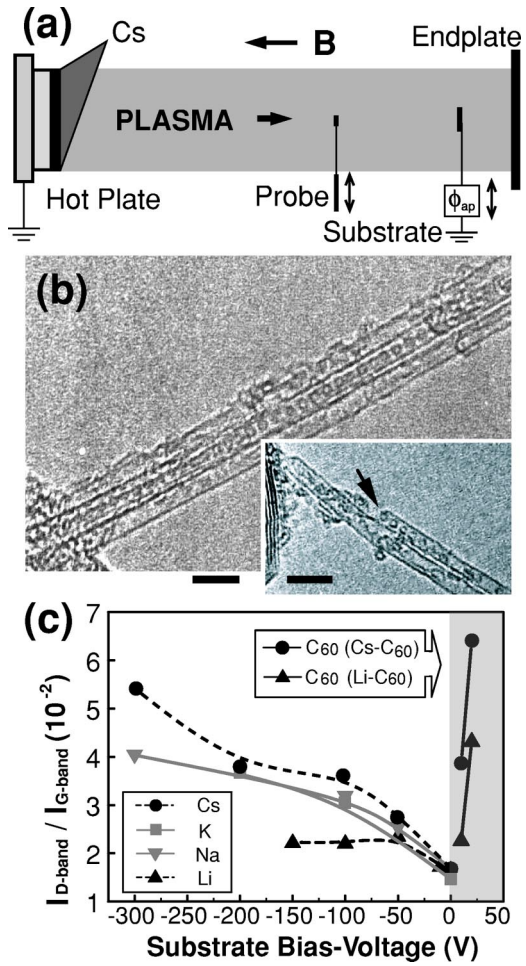

FIG. 1. (a) Experimental unit used in this study. (b) FE-TEM image showing peapods synthesized by the plasma ion irradiation method. The black arrow in the inset indicates that fullerenes are presumably encapsulated via the open end. The scale bar is 4 nm. (c) Variations of I_D/I_G values for different substrate bias voltages.

in the code SIESTA[20,21] has been successfully applied to a variety of different systems recently.[22–24] The reliability of the method is further tested for the present case by performing separate calculations on Cs_2^+ and Cs_2, as well as $[CsC_9]^-$, and comparing the results against the available data in the literature.[25,26]

III. RESULTS AND DISCUSSION

A. Structural modification and consecutive filling mechanism by plasma ion irradiation

We have previously reported[27,28] the formation of fullerene encapsulating SWNTs, so called peapods, by application of positive bias ($\phi_{ap}=20$ V) to SWNTs, using alkali-fullerene plasmas as shown in Fig. 1(b). The peapods are proved to be synthesized through consecutive open-end formation by accelerated C_{60}^- impact and encapsulation via the open ends, within the same plasma irradiation process.[27,28] This is specially denoted by a black arrow in the inset of Fig. 1(b). Recently, we have found that the fullerene encapsulation rate linearly increases with an enhancement of the plasma density.[29] For example, the peapods formation yield is raised up from 20 – 25 % and 40 – 45 %, to 60 – 70 % by the enhancement of plasma density (n_e) from $n_e \sim 10^8$ cm^{-3} and $n_e \sim 10^9$ cm^{-3}, respectively, to $n_e > 10^{10}$ cm^{-3}. This C_{60} encapsulation yield is estimated on the basis of comparing the length of encapsulating parts to the total length of clearly discernible nanotubes from many high resolved images. The images are randomly taken by field emission type transmission electron microscopy (FE-TEM, Hitachi HF-2000), which is operated at 200 kV, having a point-to-point resolution of 0.23 nm. It is reasonable that higher plasma density means increased irradiation ion-flux, which may be crucial in the enhancement of the encapsulation rate.

Our structural deformation and consecutive encapsulation mechanism mentioned above is also strongly supported by the good agreement of the TEM results with the Raman results as depicted in Fig. 1(c). Therefore, in order to evaluate the degree of structural deformation, we introduce an intensity comparison of Raman peaks (I_D/I_G, I_D: Intensity of the defect-band I_G: Intensity of the graphite-band) as a quantitative measure of SWNT structure. First, when we examine the relationship between the value of I_D/I_G and the applied substrate bias voltage, it is found that the value of I_D/I_G increases with increasing the applied bias voltage value. In other words, the degree of nanostructure disorder increases due to increased ion irradiation energy. Secondly, we have to investigate the dependence of the I_D/I_G value on the plasma density that we used at the same substrate bias voltage. The values of I_D/I_G for the C_{60} irradiation with $\phi_{ap}=10$ or 20 V in the $Li^+ - C_{60}^-$ plasma are lower than the corresponding values in the case of $Cs^+ - C_{60}^-$ plasma. Namely, the amount of structural modification increases with the enhanced C_{60} negative ion flux toward SWNTs. A more interesting fact is that the value of I_D/I_G for C_{60} irradiation by applying $\phi_{ap}=10$ or 20 V to the alkali-fullerene plasma [gray region in Fig. 1(c)] is much higher than that in the case of positive alkali-metal irradiation. Finally, from the relationship between the plasma density, the C_{60} encapsulation yield, and the I_D/I_G value, we can conjecture that the modified SWNTs structures in our experimental system are mainly produced by momentum transfer from the accelerated charged particles to the nanotubes; a fact that might contribute to yielding an enhanced encapsulation of dopants inside the SWNTs.

B. Cs encapsulation inside the SWNTs

Cs is selected as dopant because of its large diameter ($\sim$ 0.34 nm) and heavier weight as compared to other alkali metals. The latter is advantageous to make the dopants easier to detect by *Z*-contrast technique in scanning TEM (STEM), while the former is beneficial for doping only through the open end (not via the tube wall) and for the stability of the junction configuration. Thus, Cs tends to enter mainly through the open end when the tubes are relatively free of large defects in their walls, and once one Cs is blocked inside the tube from moving further, presumably by a rather small

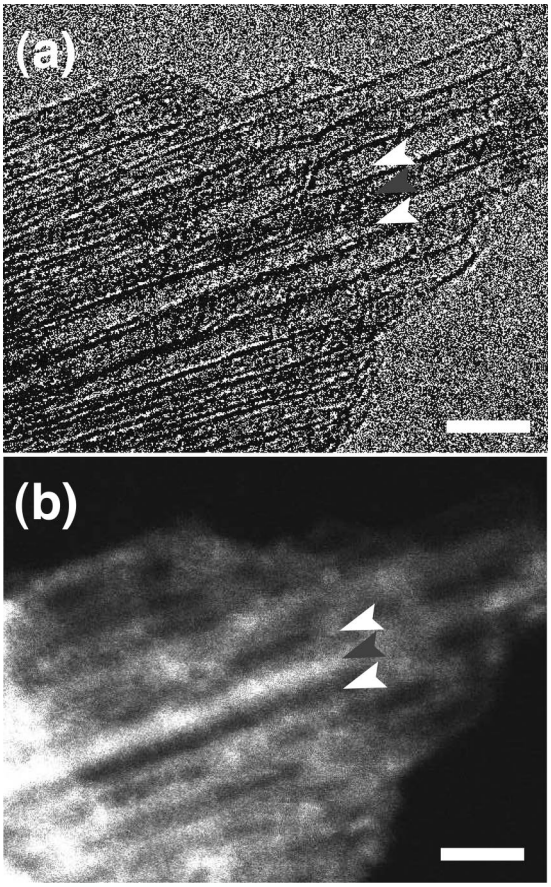

FIG. 2. (a) Bright-field STEM image of sea-urchin type SWNTs irradiated by $\phi_{ap} = -100$ V in Cs plasma. (b) Corresponding *Z*-contrast image clearly shows the partial encapsulation of Cs by contrast difference. White/black arrows in (a) and (b) indicate hollow/Cs-filled nanotubes, respectively. All scale bars correspond to 4 nm.

defect, it blocks the way for the other Cs ions as well. This may not happen for smaller dopants.

The *Z*-contrast technique, which is very useful for characterizing the spatial distribution of chemical elements at the atomic scale by STEM (Hitachi HD-2000 in our experiments),[30] is adopted to get highly reliable information from the Cs-encapsulating SWNTs. Using this technique, Fan *et al.* have recently reported that the configuration of the iodine atoms intercalated by capillary wetting method inside SWNTs is helical.[31] It is known that large contrast differences in *Z*-contrast imaging originate from the intensity differences of high-angle scattered electrons, which are proportional to the square of atomic number (Cs=55 and C=6). In our case of sea-urchin type SWNTs, the Cs encapsulating tube (indicated by black arrow), is darker than the neighboring empty tubes (white arrows) in Fig. 2(a). Tubes encapsulating Cs are distinguished as bright stripes of $\sim$ 1.5 nm diameters in Fig. 2(b). Specifically, it is evident that the positions of Cs-filled tubes in Fig. 2(a) exactly coincide with the bright lines in dark field image in Fig. 2(b).

Figure 3 reveals the difference between outside adsorption and inside encapsulation. Figure 3(a) shows a thin bundle composed of 2–3 individual nanotubes bridging two thick

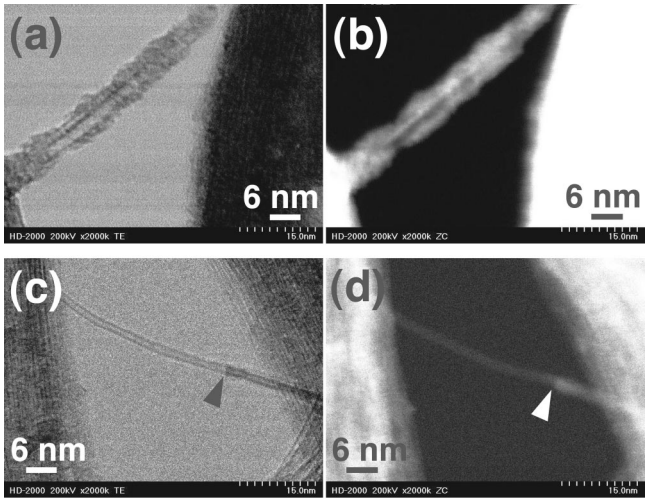

FIG. 3. (a) Bright-field STEM image of Cs adsorbed SWNTs. (b) Corresponding *Z*-contrast image of (a). (c) Cs inside filling of individual nanotube. (d) Corresponding *Z*-contrast image of (c). Arrows in (c) and (d) indicate the junction of hollow and filled regions.

bundles, which illuminates very brightly in Fig. 3(b) due to the Cs presence. On the other hand the junction point between empty (left side) and Cs-filled (right side) parts of a SWNT is clearly designated by arrows in Figs. 3(c) and 3(d). These figures imply the very important fact that Cs ions presumably do not enter through the side-wall defect, although a side-wall diffusion is predicted both experimentally and theoretically in the case of Li (Refs. 5,6) which has a smaller diameter ($\sim$ 0.15 nm) compared with that of Cs ($\sim$ 0.34 nm) or the hexagonal ring of the tube ($\sim$ 0.25 nm). If the side-wall defects, which would be produced by numerous Cs-ion bombardments, act as a window for encapsulation, we cannot explain how this local filling takes place. In other words, it is very hard to explain why Cs ions are not distributed uniformly along the entire tube. From these results, we conclude that the Cs encapsulation presumably takes place via opened ends, which are caused by momentum transfer from Cs ions to SWNTs. In this case, a small defect in the side-wall may block the movement of the Cs ions inside the tube; hence the localized junction in Figs. 3(c) and 3(d).

Figure 4 gives FE-TEM image and EDS (energy dispersive x-ray spectrometry, Norman Instruments) spectrum obtained from the samples treated with $\phi_{ap} = -100$ V in the Cs plasma. It is evidently seen that an individual and clean SWNT is partially filled with Cs. The inset in Fig. 4(a) emphasizes the encapsulated cesiums by dotting with black circles. Here, in order to obtain the more accurate compositional information, *in situ* EDS analysis is performed during the FE-TEM observation. Although we have firstly tried element mapping and line scanning, the amounts of Cs within the tubes seem to be insufficient for identification. Due to this quantitative detection limit of the EDS, the analysis is performed using the compressed electron beam (<5 nm diameter) from a very thin and isolated bundle, which inevitably yields a relatively weak intensity for the Cs spectrum

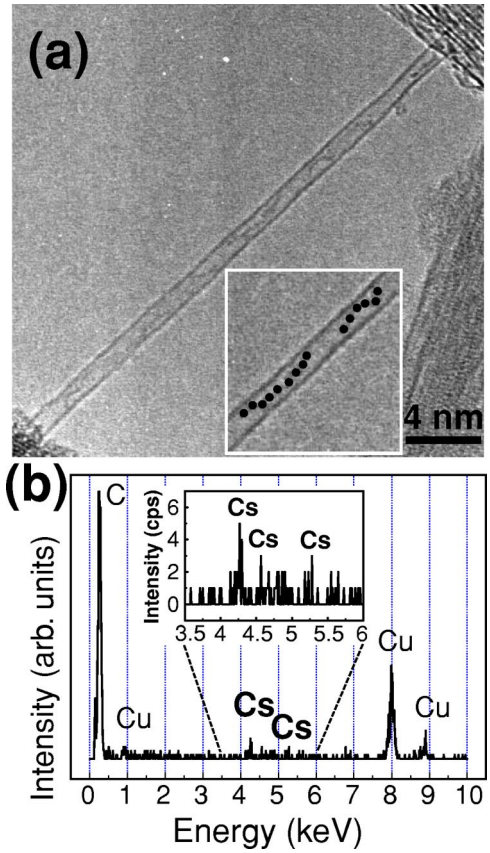

FIG. 4. FE-TEM image and EDS spectrum obtained from the samples treated with $\phi_{ap}=-100$ V in the Cs plasma. (a) A sample partially filled by Cs. The inset underlines the encapsulated cesiums by dotting with black circles. (b) EDS result reveals the Cs existence.

peak. This process permits us to confirm the Cs presence in the irradiated SWNTs as shown in Fig. 4(b).

C. Computational results of *ab initio* modeling

We consider a (10,10) armchair tube, with a radius of 6.78 Å in agreement with the experimental observations. First the potential profiles corresponding to different distances between the Cs ion/atom, located on the diagonal direction inside the tube, and the nanotube wall are determined. The results, shown in Fig. 3, indicate that there are two minima along the diagonal direction, in accordance with our previous results for the Na and K cases.[32] Each of these minima corresponds to the situation that the Cs ion/atom is separated from the tube wall by 3.0 Å. The energies of the stable configurations are -0.70 and -0.86 eV for the ionized and neutral Cs, respectively, as compared to the case that Cs ion/atom is located on the tube axis. This energy difference originates from the extra attractive force in the case of neutral Cs, resulting from the charge transfer to the carbon lattice. These results were obtained, without structure relaxation, using a portion of the tube including seven carbon rings (a carbon ring consists of all the atoms of the tube with the same longitudinal coordinate), where the C-C bonds of the open ends were contracted by ~ 0.2 Å. This is in accordance with the relaxation results, where a reduced C-C bond-length is detected at the ''clean'' open ends[33] of the tube for the bonds perpendicular to the tube axis, that indicates a change of bonding character to triple bond. In order to obtain the energetics for the relaxed structure, however, a portion of the tube, including 132 carbon atoms and resembling a bent rectangle, whose bordering dangling bonds are saturated with hydrogen atoms, is considered. Six different configurations, defined in Table I and Fig. 5, are chosen for the initial position of the Cs ion. The initial distance of the Cs ion and the nanotube wall is set to 2.7 Å, and throughout the relaxation process two rows of bordering carbon atoms, together with all the ending hydrogens, are kept fixed. The maximum force tolerance for the relaxed structures is set to 40 meV/Å. The results of the structure relaxations show that all the six configurations are local energy minima, and Cs ions are 3.0 Å away from the nanotube wall. From Table I, the energies of the inside configurations are observed to be lower than the corresponding energies of the outside configurations by $\sim$ 0.15 eV. This indicates that inside encapsulation of the Cs ions is energetically more favored as compared to the outside adsorption. This is attributed to the higher concentration of the p_z orbitals of carbon lattice inside the tube, as a result of tube curvature.

TABLE I. Energetics [eV] of Cs-ion adsorption (outside) or encapsulation (inside) above (below) the center of a hexagon, the center of a C-C bond, and a carbon atom. (The reference is different than that of Fig. 5.)

	Hexagon	C-C bond	C atom
adsorption	-0.52	-0.48	-0.47
encapsulation	-0.65	-0.65	-0.64

Considering the metallic character of the tube, and the fact that the nanotube is deposited on a metallic substrate attached to negative bias voltage, it is reasonable to conclude that the positive charges of the Cs ions are (at least partially)

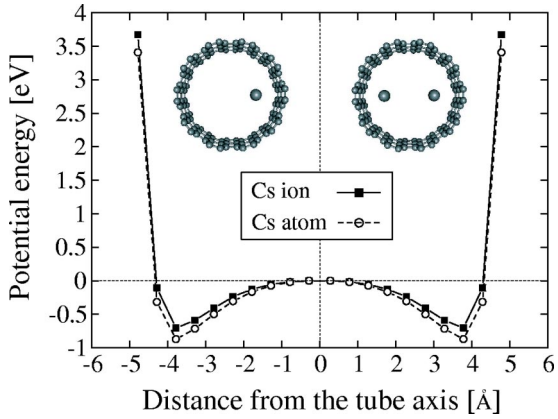

FIG. 5. Potential energy profile for a Cs ion/atom located on the diagonal direction (perpendicular to the tube axis), for different distances between the Cs ion/atom and a (10,10) nanotube wall (located at ± 6.78 Å). The stable positions are located at a distance of 3.0 Å from the wall. Inset: Schematic views of the encapsulation of Cs at one or both of the stable positions.

neutralized. This explains the observation of the combined attachment of many Cs atoms in Figs. 2(a) and 2(b); a configuration which is not possible for Cs ions due to Coulomb repulsion.

Mulliken population analysis shows that the net charge of both ionized and neutral Cs is $\sim 0.8\,e$. This indicates the electron acceptor (donor) character of Cs ion (atom) after encapsulation. The presence of a row of Cs inside one part of the tube, and not in the other part, as is seen in Figs. 2(c) and 2(d), would result in a shift of the density of states (DOS) of one part of the tube as compared to that of the other part. In Fig. 6 we show the band structures and DOSs of the pure (10,10) tube, together with two cases of light and heavy doping with neutral Cs atoms, which correspond to filling only one or both of the stable positions for Cs depicted in Fig. 3, respectively. The DOS shift in a nanotube enables us to make a doped nanotube junction, which is predicted[10] to behave as a nanodiode. The system depicted in Figs. 2(c) and 2(d) can therefore be regarded as the actual realization of such a nanoelectronic device. In calculating the data of Fig. 6, the unit cell of the nanotube includes six carbon rings. This makes the mutual Cs-Cs force equal to 60 meV/Å, taken to be small enough for assuming a stable configuration. Two of the interesting features of Fig. 6 are: First, the formation of one and two nearly flat bands for the cases of light and heavy doping, respectively, within the conduction bands of the tube. Second, the alignment of the Fermi energy with one of the van Hove singularities of the DOS of the heavily doped tube. This latter feature is of interest as it indicates the superconducting tendency as a result of heavy doping with alkali metals.

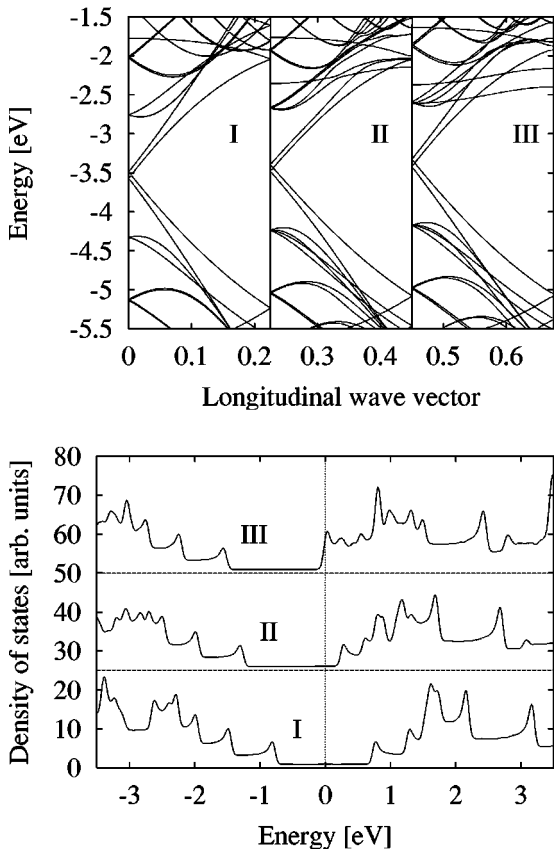

FIG. 6. The band structures (top) and density of states (DOS) (bottom) for a (10,10) tube which is pure (I) and doped with a single (II) and two (III) Cs atom(s) per six carbon rings. For the band structures, Fermi energies are located at -3.53, -2.95, and -2.63 eV, for the cases I, II, and III respectively. For the DOS curves, Fermi energies are shifted to zero.

IV. CONCLUSIONS

In conclusion, the formation of Cs-encapsulating SWNTs is verified experimentally, and characterized theoretically by *ab initio* investigations. We find that the inside doping is more favorable compared to the outside doping. Using the *Z*-contrast technique, the plasma-ion irradiation is shown to be an efficient method for insertion of the metal atoms in the core of the tubes. Our results suggest that the plasma-ion irradiation is a good candidate for producing more intricate quasi-one-dimensional nanodevices, such as intratube junctions, via encapsulating selected ions.

ACKNOWLEDGMENTS

The authors thank P. Ordejón for fruitful comments. Part of this work was carried out under the Cooperative Research Project Program of the Research Institute of Electrical Communication, Tohoku University. This work was also supported by a Grant-in-Aid for Scientific Research from the Ministry of Education, Culture, Sports, Science, and Technology, Japan.

*E-mail address: hatak17@ec.ecei.tohoku.ac.jp

[1] R. S. Lee, H. J. Kim, J. E. Fischer, A. Thess, and R. E. Smalley, Nature (London) **388**, 255 (1997).

[2] A. A. Farajian and M. Mikami, J. Phys.: Condens. Matter **13**, 8049 (2001).

[3] J. Sloan, A. I. Kirkland, J. L. Hutchison, and M. L. H. Green, Chem. Commun. **2002** 1319 (2002).

[4] A. M. Rao, P. C. Eklund, S. Bandow, A. Thess, and R. E. Smalley, Nature (London) **388**, 257 (1997).

[5] H. Shimoda, B. Gao, X. P. Tang, A. Kleinhammes, L. Fleming, Y. Wu, and O. Zhou, Phys. Rev. Lett. **88**, 015502 (2002).

[6] V. Meunier, J. Kephart, C. Roland, and J. Bernholc, Phys. Rev. Lett. **88**, 075506 (2002).

[7] S. Suzuki, C. Bower, and O. Zhou, Chem. Phys. Lett. **285**, 230 (2000).

[8] S. Suzuki, C. Bower, Y. Watanabe, and O. Zhou, Appl. Phys. Lett. **76**, 4007 (2000).

[9] K. Esfarjani, A. A. Farajian, Y. Hashi, and Y. Kawazoe, Appl. Phys. Lett. **74**, 79 (1999).

[10] A. A. Farajian, K. Esfarjani, and Y. Kawazoe, Phys. Rev. Lett. **82**, 5084 (1999).

[11] Z. Wan, J. F. Christian, and S. L. Anderson, Phys. Rev. Lett. **69**, 1352 (1992).

[12] R. Tellgmann, N. Krawez, S. -H. Lin, I. V. Hertel, and E. E. B. Campbell, Nature (London) **382**, 407 (1996).

[13] T. Weiske, D. K. Böhme, and H. Schwarz, J. Phys. Chem. **95**, 8451 (1991).
[14] M. M. Ross and J. H. Callahan, J. Phys. Chem. **95**, 5720 (1991).
[15] D. E. Giblin, M. L. Gross, M. Saunders, H. J. Vazquez, and R. Z. Cross, J. Am. Chem. Soc. **119**, 9883 (1997).
[16] K. Tohji, T. Goto, H. Takahashi, Y. Shinoda, N. Shimizu, B. Jeyadevan, I. Matsuoka, Y. Saito, A. Kasuya, T. Ohsuna, K. Hiraga, and Y. Nishina, Nature (London) **383**, 679 (1996).
[17] N. Sato, T. Mieno, T. Hirata, Y. Yagi, R. Hatakeyama, and S. Iizuka, Phys. Plasmas **1**, 3480 (1994).
[18] N. Troullier and J. L. Martins, Phys. Rev. B **43**, 1993 (1991).
[19] J. P. Perdew, K. Burke, and M. Ernzerhof, Phys. Rev. Lett. **77**, 3865 (1996).
[20] P. Ordejón, E. Artacho, and J. M. Soler, Phys. Rev. B **53**, R10 441 (1996).
[21] D. Sanchez-Portal, P. Ordejón, E. Artacho, and J. M. Soler, Int. J. Quantum Chem. **65**, 453 (1997).
[22] S. Reich, C. Thomsen, and P. Ordejón, Phys. Rev. B **65**, 153407 (2002).
[23] S. Reich, J. Maultzsch, C. Thomsen, and P. Ordejón, Phys. Rev. B **66**, 035412 (2002).
[24] A. A. Farajian, M. Mikami, P. Ordejón, and K. Tanabe, J. Chem. Phys. **115**, 6401 (2001).
[25] I. Moullet, W. Andreoni, and P. Giannozzi, J. Chem. Phys. **90**, 7306 (1989).
[26] A. Dreuw and L. S. Cederbaum, J. Chem. Phys. **111**, 1467 (1999).
[27] G. -H. Jeong, R. Hatakeyama, T. Hirata, K. Tohji, K. Motomiya, N. Sato, and Y. Kawazoe, Appl. Phys. Lett. **89**, 4213 (2001).
[28] G. -H. Jeong, T. Hirata, R. Hatakeyama, K. Tohji, and K. Motomiya, Carbon **40**, 2247 (2002).
[29] R. Hatakeyama, T. Hirata, and G. -H. Jeong, Plasma Sources Sci. Technol. (to be published).
[30] URL http://www.hitachi-hitec.com/science/english/product/tem/hd2000.html
[31] X. Fan, E. C. Dickey, P. C. Eklund, K. A. Williams, L. Grigorian, R. Buczko, S. T. Pantelides, and S. J. Pennycook, Phys. Rev. Lett. **84**, 4621 (2000).
[32] A. A. Farajian, K. Ohno, K. Esfarjani, Y. Maruyama, and Y. Kawazoe, J. Chem. Phys. **111**, 2164 (1999).
[33] By ''clean open end'' we mean a clean-cut end where all the bordering C-C bonds of the (10,10) tube lie within the same plane which is perpendicular to the tube axis.